Visual Neuroscience (1989), 2, 553–564. Printed in the USA

Signal integration at the pedicle of turtle cone photoreceptors: An anatomical and electrophysiological study

ERIC M. LASATER,[1] RICHARD A. NORMANN,[2] AND HELGA KOLB[1]

[1]Departments of Physiology and Ophthalmology, University of Utah, School of Medicine, Salt Lake City
[2]Departments of Bioengineering, Physiology, and Ophthalmology, University of Utah, School of Medicine, Salt Lake City

(RECEIVED October 19, 1988; ACCEPTED March 8, 1989)

Abstract

The morphology of the axon which connects the cell body and pedicle of turtle cone photoreceptors was studied by light and electron microscopy. The axon which contains numerous synaptic vesicles, some endoplasmic reticulum, and a few cisternae is basically filled with cytoplasm. The length of the axon is related to the class of cone and varies slightly with retinal location, with axons as short as 3–6 μm found in red cones, and as long as 60 μm in cones containing colorless oil droplets. By simultaneously voltage clamping the cell body and pedicle regions of single isolated cones, we measured the longitudinal axonal resistance and the cell body and pedicle membrane resistances. For each cell studied, the axonal resistance of cones with short axons was lower than the cell and pedicle membrane resistances. Thus, the cell can be considered to be an isopotential structure. However, in some cones with long axons, the axonal, cell body, and pedicle resistances were comparable. The pedicles of these cones, therefore, could act like summing points and may provide a locus for spatial signal integration. Electrical coupling between the principal and accessory members of double cones was also studied. Electron-microscopic observation of the membrane junction between the apposed inner segments of the double cones in the intact retina show narrow segments which resemble gap junctions. However, in every double cone studied in culture, passing currents into one member of the double cone did not result in measurable current flow in the adjacent cell. Thus, the two members of the double cone, isolated from the turtle retina, are not electrically coupled.

Keywords: Cone photoreceptor, Voltage clamp, Isolated cells, Input resistance, Cell body-pedicle coupling

INTRODUCTION

A given vertebrate photoreceptor responds to absorption of photons in its own outer segment and also in the outer segments of neighboring photoreceptors. The pathways by which information about photon absorption in neighboring photoreceptors is shared between photoreceptors have yet to be fully elucidated, and may consist of chemical and/or electrical synapses between photoreceptor telodendria, the close appositions and possibility of gap junctions between members of double cones, and interneuronal communication mediated by the horizontal cell. Furthermore, the structure of the photoreceptor itself may provide a means for spatial integration of information; the axon connecting the cell body and the synaptic terminal of the photoreceptor might strongly couple or alternatively loosely couple these two regions of the photoreceptor. If the latter were the case, the synaptic ending of the photoreceptor could act as a "summing point" where a variety of inputs to the terminal were temporally and spatially integrated.

There are observations which argue for such a view of signal integration at the synaptic endings of photoreceptors. The experiments of Hagins et al. (1970) suggest that the cell body and synaptic ending may not be isopotential, that the membrane voltage response at the synaptic ending may be only one-tenth the size of the response at the cell body. Furthermore, the large receptive fields of horizontal cells are believed to provide the inhibitory surround observed in bipolar cells (Werblin & Dowling, 1969; Naka & Nye, 1971; Kaneko, 1973). One theory proposes that this surround is conveyed to the bipolar cell via a negative feedback pathway onto the cone photoreceptors (Baylor et al., 1971) which drive the bipolar cell (Toyoda & Kujiraoka, 1982). However, the surround effect in bipolar cells is profound while that observed in cones is much more subtle (Baylor et al., 1971), a subtlety which could be explained by a loose coupling of signals between cone cell bodies and their synaptic regions (the cone pedicle). Since our understanding of

Reprint requests to: Eric M. Lasater, Department of Physiology, University of Utah School of Medicine, 410 Chipeta Way, Salt Lake City, Utah 84108, USA.

cone physiology is a result of intracellular recordings which are most probably made in the cell bodies or inner segments of cones, these recordings would be expected to reflect more directly photon absorption in the outer segment of the impaled cone than events in the synaptic pedicle. Horizontal cell feedback, however, would predominate at the pedicle. Unfortunately, because of the smaller volumes of the synaptic ending of the cone pedicle, it is unlikely that we will ever be able to impale a pedicle in the intact retina with an intracellular electrode, identify it as such, and verify this hypothesis.

There are considerations which would argue for the view that the cell body and pedicle of the cone are more isopotential. Estimates of the cytoplasmic resistance of the axon indicate that this should be in the 4–40 MΩ range, a relatively low value compared to the expected membrane resistances of the cell body and pedicle. However, this estimate of axonal longitudinal resistance is subject to large errors due to the variability in published reports on the dimensions and microstructural morphology of the axon. Ohtsuka and Kouyama (1986) report that the diameter of the turtle cone axon is less than 1 μm, while Kolb and Jones (1982, 1987) report that the diameter is in the 1–2 μm range. Furthermore, in the turtle retina the length of the axon appears to depend upon a number of parameters such as the position of the cell in the retinal mosaic and the type of cone. Kolb and Jones (1987) have reported that the lengths of cone axons vary from 5–60 μm. This admittedly very rough estimate of longitudinal axonal resistance is based upon an assumed cytoplasmic resistivity of 2 Ω-m, a value found in invertebrate axoplasm (Schanne & Ruiz P.-Ceretti, 1978). A direct measurement of axonal longitudinal resistance and cell body and pedicle membrane resistances would answer the question concerning the extent of coupling between the cell body and pedicle of the cone.

In the following experiments, we have quantified the dimensions of cone axons and estimated their axial resistances. We also measured and found no electrical coupling between the members of double cones.

Methods

Isolation procedure

Eyes were removed from *Pseudemys scripta elegans* turtles (carapace length 6–8 in.), hemisected, and the retinas removed by scooping from the eyecup. Isolated retinas were placed in 10 ml of modified Leibowitz's L-15 tissue culture medium containing 2.2 mg of papain (24 u/mg) for 45 min. Following this period of papain incubation, the retinas were washed once and cells dispersed into tissue-culture dishes by trituration with Pasteur pipettes. While retinal neurons other than cones could be maintained in seemingly good condition for a number of days, cones began to show swelling with a reduced index of refraction about 6–8 h after isolation.

Morphological techniques

Light microscopy

Photoreceptors were isolated and dispersed in tissue-culture dishes as described in the above isolation procedure. The cultures were viewed under white and fluorescent light in an Olympus fixed-stage microscope and photographed with Kodak ASA 400 film using a 40X objective. Ultraviolet light using a 330–420-nm stimulating filter and a 450-nm blocking filter was used to check on the identity of cones with colorless oil droplets (see Kolb & Jones, 1987). Identification of the cone spectral type was made based on its oil droplet color and fluorescence while the length of the axon was measured from the projected color slides. The thickness of the axon was difficult to measure accurately under these conditions and therefore measurements of axon diameters were made from electron micrographs of cross-sectioned photoreceptor axons in fixed retinal tissue.

Electron microscopy

The procedures for fixation, embedding, and thin sectioning are exactly as described in Kolb and Jones (1984). Retinas were fixed in either chrome-osmium fixative (Dalton, 1955) or in a double aldehyde (1% formaldehyde, 2% glutaraldehyde) fixative, en bloc stained in 1% uranyl acetate in 0.05 M sodium acetate, and dehydrated and embedded in standard fashion. Ultrathin sections cut vertically or tangentially through various levels of the photoreceptor mosaic were examined and photographed in the electron microscope for later measurement of cross-sectional diameters or vertical lengths of the axons of cone photoreceptors.

No corrections were made for cell shrinkage in either the light or electron micrographic measurements.

Recording procedure

Voltage-clamp experiments were carried out using the technique of whole-cell patch clamp as described by Hamill et al. (1981). Electrodes were fabricated from borosilicate glass with a Kopf Model 750 electrode puller employing a two-stage pull. The tips of the electrodes were then heat polished. The resultant patch electrodes, when filled with the intracellular solution (see below), had resistances, measured in Ringer's, of 4–10 MΩ.

A chlorided silver wire connected the bath to ground and a similar wire connected the electrode to the voltage-clamp headstage. Junction potentials between ground and the input were nulled by an offset voltage adjusted to make the output current zero when the electrode was sealed to the cell membrane. Junction potential drift over the course of an experiment was almost negligible. The series resistance of the electrodes was electronically compensated.

Membrane currents were amplified and recorded on a thermal strip-chart recorder (d.c. to 110 Hz frequency response). Measurements were then made directly from the chart recordings. Some data was collected on-line with a Keithley System 470 (Keithley Instruments, Cleveland, OH) data collection system controlled by an IBM-AT personal computer. The data was low-pass filtered at 5 kHz with a four pole Butterworth filter before being sampled at a rate of 29 kHz. This data was analyzed off-line.

Experimental solutions

Prior to each experiment, the L-15 solution bathing the cells was replaced with a Ringer's solution equilibrated with O_2 and adjusted to pH 7.6. The Ringer's consisted of 130 mM NaCl, 3.0 mM KCl, 2.1 mM $CaCl_2$, 1.2 mM $MgCl_2$, 0.44 mM KH_2PO_4, 1.2 mM $NaHCO_3$, 10 mM glucose, and 10 mM N-2-hydroxyethylpiperazine-N′-2-ethane-sulfonic acid (HEPES).

The patch pipettes used for recording in these experiments were filled with a solution consisting of 84 mM potassium

gluconate and 36 mM KF, 4 mM KCl, 1 mM $CaCl_2$, 1 mM MgATP, 11 mM EGTA, and 10 mM HEPES titrated to a pH of 7.4 with NaOH. The free Ca^{2+} concentration of this solution was calculated to be 6.7×10^{-9} M.

Experimental procedure

A suitable cell was first located in an inverted microscope, then photographed with a 35-mm camera. The images of some cells were captured and stored digitally using a frame grabber (Imaging Technology Inc., Woburn, MA) in conjunction with a Hitachi CCTV camera (Hitachi Denshi Ltd., Tokyo, Japan). At 400X, the system had a resolution of about ± 0.25 μm. These digitized images were used to make some of the measurements of pedicle and cell body sizes as well as lengths of axons. Two patch-clamp electrodes were then positioned on the cell; one at the pedicle and one at the cell body. Negative pressure was applied to the lumen of the patch pipette to effect a seal. A short period of time, 10–20 s, was allowed to pass for the equilibration of the pipette contents with the pipette tip. During this time, capacity compensation was maximized and the junction potential was nulled. Further negative pressure was then applied to rupture the cell membrane and gain access to the cell's interior. Most cells were held at −70 mV. Several experiments on cells held at −35 mV indicated that holding potential did not affect these particular experimental results. Hyperpolarizing and depolarizing, 80-ms duration, voltage-command pulses were passed through one electrode either to the pedicle or cell body and the resulting currents flowing through both electrodes were recorded. Voltage-command pulses spanned the range from −170 to +30 mV in 10-mV increments. After the full range of voltages were covered, the voltage-command regime was delivered to the other electrode. Finally, both electrodes were stepped with equal voltage commands and both current responses recorded. In the data analysis, many of the cell body and pedicle resistance calculations were made for the 50-mV command. The amplitudes of the current pulses were measured at the end of the pulse and thus the measurements represent steady-state current levels.

Results

Morphology of cone photoreceptors and axons

Figure 1A shows a red cone photoreceptor as seen in isolation in tissue culture. The outer segment, oil droplet, inner segment, cell body, axon, and pedicle are clear morphological aspects of this cell type. In transverse electron-microscope sections through the entire length of a cone *in situ*, more details of the organelles can be seen (Fig. 1B). The ultrastructural appearance of the different spectral cone types in turtle have been described before (Kolb & Jones, 1982, 1987). However, an important feature of cones of the turtle retina, pertinent perhaps to the electrical measurements to be described in this paper, is the relationship of the nuclear region of the cell body to the axon. Note that the nucleus of turtle cones occupies the lower end of the cell body sitting like a ball in a chalice above the point of emergence of the narrow axon. The cytoplasm of the cone cell body is restricted to an extremely narrow rim in this region (arrows, Fig. 1B).

Electron-microscopic examination of cone axons of the turtle retina show that these structures are filled with cytoplasmic matrix material in which small cisternae and synaptic vesicles are floating (Figs. 2A–C). The cisternae are mostly smooth membranes but in the vicinity of the cell body region of the axon some rough endoplasmic reticulum is also visible, possibly deriving from the sparse Golgi and Nissl complex below the nucleus of the cell (Fig. 2A). What appear to be synaptic vesicles occur in the middle to lower end of the axon (double arrows, Fig. 2A) before the axon enlarges to become the cone pedicle which is, of course, filled with synaptic vesicles in the vertebrate photoreceptor. Cross sections through the axons (Figs. 2B–C) show a similar ultrastructural appearance. The whole axon is ensheathed by Müller cell processes and is thus isolated from neighboring cone axons, or, in the case of the double cone, even from the axon of its partner cone.

Dimensions of cone photoreceptor axons

The lengths of axons of turtle cones are a function of the location of the cells in the retina, i.e. in the visual streak *versus* near or far periphery, and also depend on the spectral type of cone. The cone axon illustrated in Fig. 1B is that of a red single cone close to the visual streak region (within 250 μm) and, as can be seen, measures 6.2 μm in length and 1.3 μm in diameter. Measuring the cross sections of 50 axons in similar electron-microscopic views as shown in Figs. 2B and C, we found the dimensions to be very uniform at a mean dimension of 1.3 μm (S.D. = ±0.07).

Identification of spectral type of cone and a concomitant measurement of the axon length was best achieved in the isolated photoreceptor preparations in tissue culture (cells such as in Fig. 1A), viewed with the inverted light microscope. The different spectral types of cones could be identified by their oil droplet color as follows: 1) red single cones have large sized red oil droplets; 2) green single cones have large yellow oil droplets; 3) double cones have two closely attached members, the principal of which contains a large orange oil droplet and the accessory a pale yellow pigmentation in place of the oil droplet; 4) blue single cones (called FC cones by Kolb & Jones, 1987) have large colorless oil droplets that fluoresce under ultraviolet (UV) stimulation; and 5) possible ultraviolet sensitive cones (called CC cones by Kolb & Jones, 1987) have small colorless oil droplets which do not fluoresce with UV stimulation.

The results of the measurements of axon lengths and diameters on 200 isolated photoreceptors are shown in Table 1. Because in an isolated photoreceptor preparation the cells are a mix from all parts of the retina, cells with very small diameter inner segments and tiny oil droplets were considered to be

Table 1. *Axon dimensions of different cone photoreceptor types of the turtle retina based on light microscopy*

Type of cone	Periphery Axon Length (μm)	Visual Streak Axon Length (μm)	Axon Diameter (μm)
Red single	$x = 3.1$, *sd* 1.6	$x = 6.3$, *sd* 2.1	1.0–1.5
Green single	$x = 5.5$, *sd* 3.4	$x = 8.0$, *sd* 2.6	1.0–1.5
Double cone	$x = 6.3$, *sd* 5.4	$x = 8.0$, *sd* 2.9	1.0–1.5
Blue single FC cone	$x = 12$, *sd* 4.2	$x = 14.4$, *sd* 5.3	1.0–1.5
CC cone	$x = 22$, *sd* 4.8	$x = 30$, *sd* 5.6	1.0–1.5

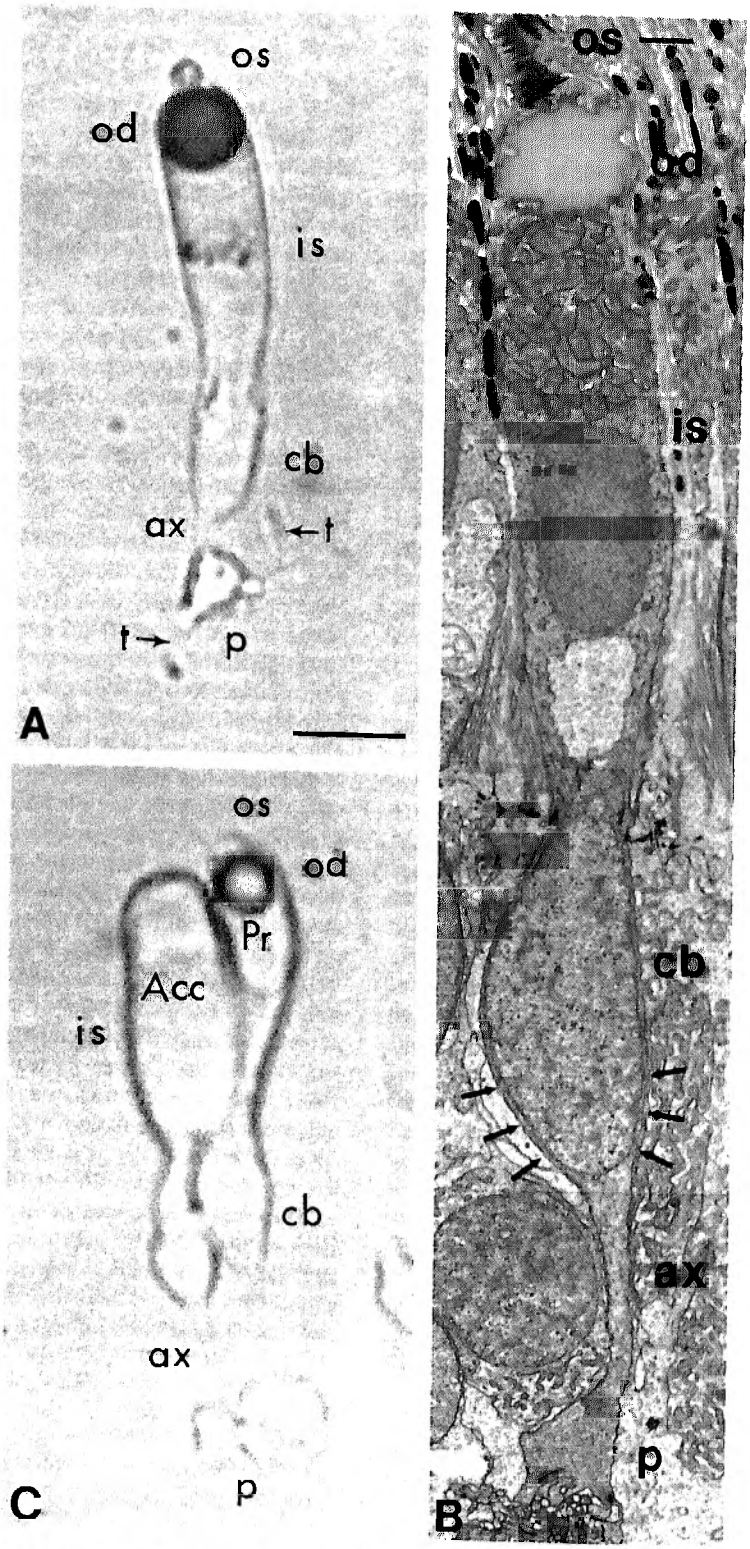

Fig. 1. A, light micrograph showing an isolated turtle red cone in cell culture. The cell has good intact morphology showing the presence of a piece of the outer segment (os), the dark red oil droplet (od), a large inner segment (is), a cell body (cb), short thin axon (ax), and a pedicle (p) that has remnants of telodendria (t, arrows) radiating from it. Scale bar = 10 μm for both A and C. B, electron micrograph of a single cone in the intact retina *in situ*. Better details of the photoreceptor organelles can be seen. Note that the nucleus of the cell body (cb) is surrounded by a very thin rim of cytoplasm (arrows) and sits like a ball in a chalice above the axon (ax) leading to the pedicle (p). Scale bar = 2 μm. C, a double cone of the turbie retina as seen in cell culture. The principal (Pr) and accessory (Acc) members of the double cone remain adhered together along their inner segments (is) and cell body (cb) regions. An outer segment (os) and an orange oil droplet (od) is present in the principal cone only. The axons (ax) and pedicles (p) of both members also remain intact.

from the visual streak and bigger cells were considered peripheral cells. As can be seen from Table 1, the red single cones typically have the shortest axons with green singles, double cones, blue singles, and clear colorless droplet cones having progressively longer axons. In general, the cones of the visual streak have slightly longer axons than peripheral cells. The commonest cones of the turtle retina are the red singles followed by the double cones and green single cones. Blue single cones are less frequent and the CC cone (UV cone?) is seen very rarely (Kolb & Jones, 1987). Therefore, the commonest cone axon lengths found in the turtle retina would be 3–6 μm with 1.3-μm diameter as the average.

Patch-clamp measurements of isolated turtle cones

Single cones

The analysis of the data described below was performed based upon a simplifying "lumped model" of the major conductances of the cone. We have combined all light modulated and leakage membrane conductances of the outer segment and

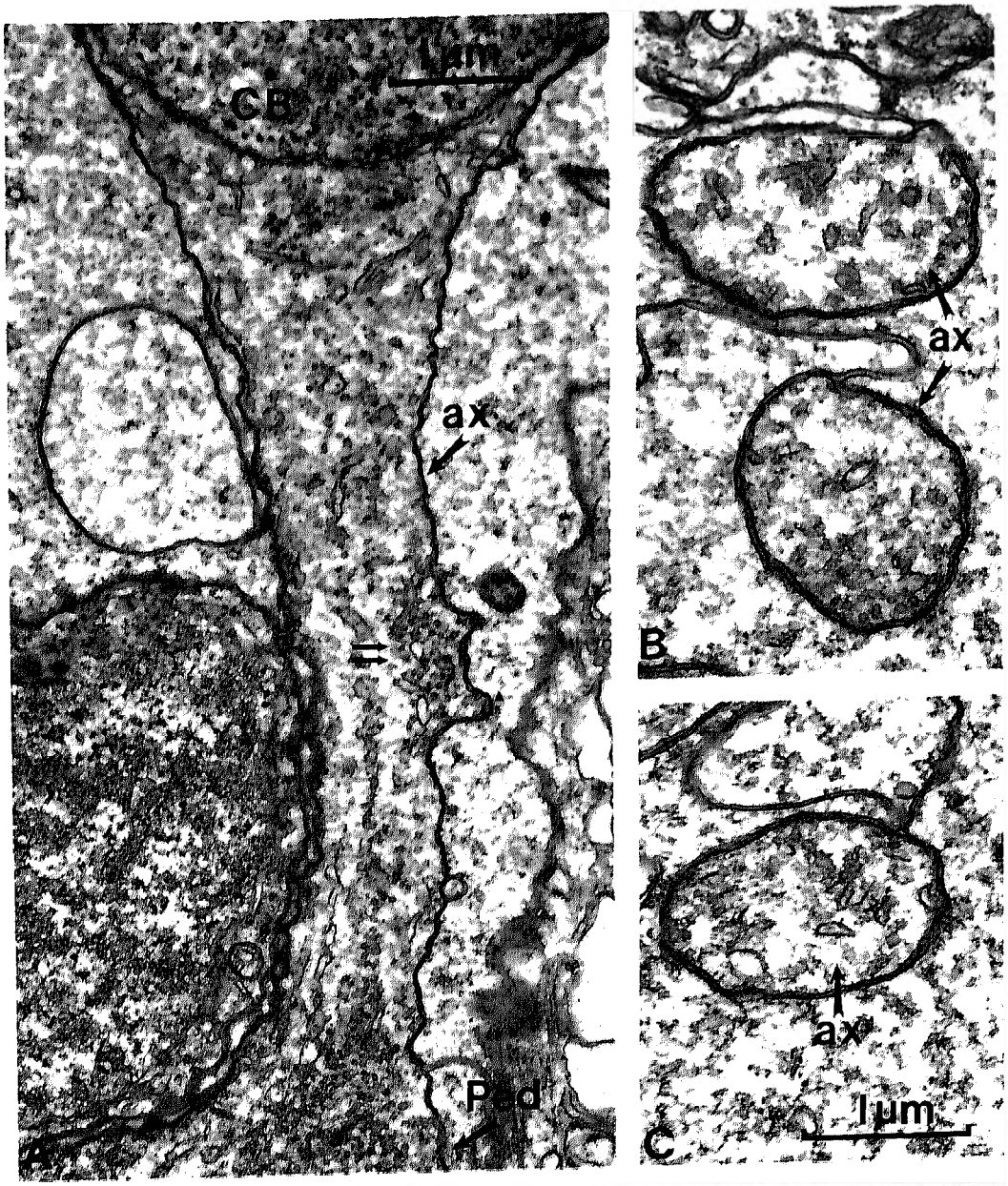

Fig. 2. A, electron micrograph showing a vertical view of the cone axon at high magnification. The axon (ax, arrow) contains cytoplasm, and a few cisternae and synaptic vesicles (double arrows). The Golgi and Nissl substance is sparse below the nucleus of the cell body where the axon narrows gradually from the cell body. Synaptic vesicles fill the pedicle (Ped, arrow). Müller cell processes ensheath the whole cone. Scale bar = 1 μm. B, C, tangential sections through the cone axons (ax, arrows) in the outer nuclear layer. The cytoplasm, cisternae, and occasional vesicles are visible. The axons are ensheathed by paler Müller cell processes. Scale bar = 1 μm for both B and C.

cell body into a single lumped resistance, R_{cb}. We have combined all ionic membrane conductances of the pedicle and telodendria into another lumped resistance, R_p. Finally, we have connected these two lumped resistances with the longitudinal axonal resistance, R_a. In this simplified model, we have assumed that the membrane resistance of the axon is infinite.

Axonal resistance of single cones. The axonal resistance of isolated cones was studied with two patch-clamp electrodes; one applied to the cell body and one applied to the pedicle. One of the two electrodes was given a voltage-command step, ΔV, and the current flowing in each electrode, ΔI, as a result of the voltage step was recorded. This recording paradigm was chosen because it allows the longitudinal resistance of the axon to be directly determined from the ratio of the size of the voltage step to the size of the current flow in the nonvoltage stepped member. For example, if one is voltage stepping the cell body, ΔV_{cb}, and measuring the current in the pedicle, ΔI_p, the resistance of the axon is given by

$$R_{\text{axon}} = \Delta V_{cb}/\Delta I_p. \quad (1)$$

Furthermore, the current-measuring electrode clamps the membrane potential at the recording site. Thus, the change in current resulting from the voltage step applied to the voltage-command electrode does not reflect any contribution from confounding voltage-dependent membrane conductances in the region of the current-measuring electrode. In this analysis, we have corrected our results for electrode resistances. The results of applying this voltage-stepping experiment to determine the longitudinal resistance of the axon are shown in Fig. 3. In this figure, the current response in the pedicle is plotted as a function of the amplitude of the voltage step delivered to the cell body. It is seen in this figure that the longitudinal axonal resistance was ohmic, with a resistance of 46 MΩ. The axonal resistance of this cone was alternatively determined to be 56 MΩ by stepping the pedicle and recording the current flow in the cell body (not shown). This type of experiment was conducted in 20 single cones, and in no case did the conductance of the axon appear to be voltage dependent. In most other cones, as in this example, the axonal resistances measured by stepping either the pedicle or the cell body were similar, usually within 10–20% of each other. The axonal resistances of 12 of these cones are tabulated in Table 2.

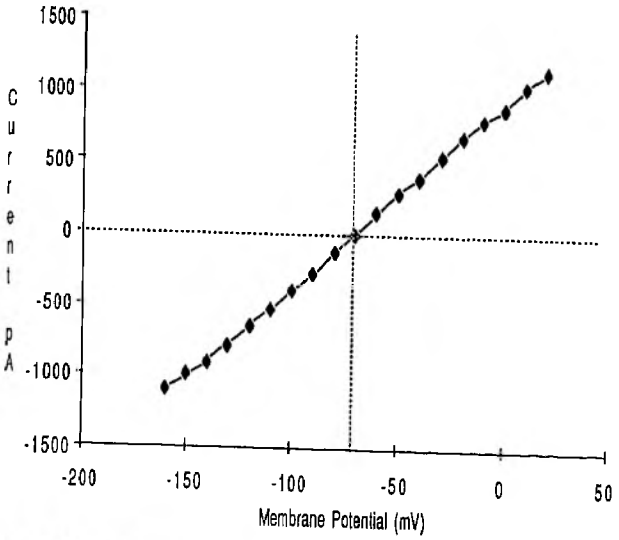

Fig. 3. Current response measured in a pedicle due to voltage steps in the cell body. The abscissa represents the size of the voltage step and the magnitude of the resultant current flow into the pedicle is plotted on the ordinate. The horizontal and vertical dotted lines represent the zero current level and the holding potential, respectively. The plot is linear, indicating an ohmic axonal resistance. The cone was held at a membrane potential of −70 mV.

Coupling of cell body and pedicle. The extent of coupling between the cell body and the pedicle can be determined in a qualitative sense by examining the size of the currents which flow in the cell body and in the pedicle in response to stepping the voltage at either site. In a cell with strongly coupled cell body and pedicle, virtually all of the current injected into one part of the cell will be recorded at the other site. In a loosely coupled cell, a large difference in these currents will be observed. In Fig. 4 are shown the cell body and pedicle currents (for one cell) which flowed as a result of voltage stepping the cell body with a variety of step sizes. In this figure, the currents flowing in the cell body are indicated with the filled bars, and the inverse of the currents flowing in the pedicle are indicated with the stippled bars. It is clear from this figure that currents of very similar amplitude were recorded at each site, which indicates that the two parts of the cell are quite strongly coupled to each other. In a more quantitative approach, the coupling coefficient (CC_a) between the cell body and pedicle can be determined. It is simply the ratio of the current measured in the noncommanded region to the current generated by the command step. For example,

$$CC_a = \Delta I_p/\Delta I_{cb} \text{ (for a voltage-stepped cell body)}. \quad (2)$$

The cell of Fig. 4 had a coupling coefficient of 0.95 (average of current responses to ± 50-mV voltage commands). For cells with axons less than 7-μM long ($n = 8$), the average coupling coefficient was 0.888 (± 0.09 S.D.), while for cells with axons of length 7-μm long or greater ($n = 6$), the average coupling coefficient was 0.707 (± 0.21 S.D..). These coupling coef-

Table 2. *Axonal resistance (in megohms) measured by stepping pedicle or cell body as a function of oil droplet color and axon length*

Cell I.D.	Axon Resistance Step Pedicle	Axon Resistance Step Cell Body	Oil Droplet Color	Axon Length (μm)
1	40	36	red	2.2
2	114	121	red	7
3	23	20	red	?
4	56	46	orange	1
5	91	79	orange	3
6	48	48	accessory	3
7	36	35	orange	13
8	38	40	orange	7
9	217	256	clear	9
10	182	307	clear	21
11	368	213	red	5
12	54	57	orange	1.4

ficients suggest a relationship between axon length and cell body–pedicle coupling. However, a larger sample size would be required to unequivocally determine this relationship.

Membrane resistances of cell body and pedicle. An estimate of cell body and pedicle membrane resistances can be obtained by stepping both cell body and pedicle simultaneously with the same size voltage step. With this paradigm, no current flows through the axon connecting the cell body and pedicle, and the currents measured with each electrode reflect the membrane resistances at each recording site. When this technique was used, the resistances of both the cell body and the pedicle were seen to be voltage dependent. Figure 5 shows the current–voltage relations for the cell body and pedicle of a cone studied in this manner. Using this technique, the average cell body resistance (measured with +50-mV command steps) was 707 (± 523 S.D.) MΩ and the average pedicle resistance was 796 (±903 S.D.) MΩ ($n = 14$).

Voltage and time dependency of membrane conductances. The voltage-dependent membrane conductances illustrated in Fig. 5 were also time dependent. The time dependencies of these conductances can be appreciated by recording the current responses of the cell body and pedicle on a faster time base. Typical current responses of a cone cell body to a series of hyperpolarizing and depolarizing steps (each 20 mV larger than the preceding voltage command) are shown in Fig. 6. The figure shows the current responses to voltage commands applied simultaneously to both pedicle and cell body. Although not examined in detail, these voltage-gated conductances appear similar to those seen in tiger salamander cones (Attwell et al., 1982) but with less rectification.

Double cones

Morphology of the membrane appositions between inner segments of double cones. Double cones in the turtle retina consist of principal and accessory cones closely adhering together so that in the tissue-culture procedures used here they always isolate from the retina as a pair with two cell bodies and two cone pedicles (Fig. 1C). By electron microscopy, we have determined that the only points of adhesion between the two members of the double cones are along the length of the inner segments. The outer segments and the axons of the two members are separated by Müller-cell ciliary processes in the former position and encased by Müller cell processes in the latter (Kolb & Jones, 1982). The question has been raised as to whether the inner segments of double cone members are electrically coupled by these gap junctions.

Figure 7A shows a cross section of a double cone at the level of the fins from the pair of inner segments which is at a level of the inner segments just above the outer limiting membrane of the retina. The nucleus of the accessory cone (Fig. 7A, Acc) projects up into the inner segment at this region of fins in this example, while the principal cone (Fig. 7A, Pr) exhibits an organelle-filled inner segment. The cell membranes of the two cells are highly convoluted but have no intervening Müller cell processes between them. Higher magnification of the convoluted adhering membranes shows that they consist of narrow and wide segments of membrane spacing. The wide segments are wider (50 nm) than normal membrane separation for two aligned cell membranes (20 nm), while the narrow gap segments are close enough to be classified as gap junctions (2–3 nm) (Fig. 7B). Serial reconstructions or freeze-fracture images are needed to adequately determine the geometry of these small narrow gap segments. However, our impression from oblique views in the thin sections is that these narrow gap segments are long and thin (750 nm × 125 nm) and aligned along the length of the attached inner segments of the principal and accessory cones.

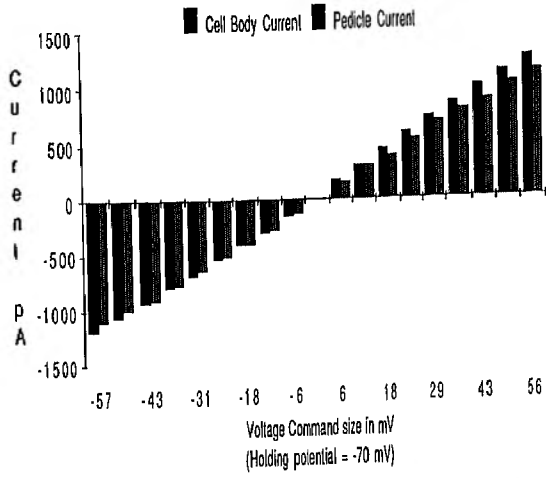

Fig. 4. A graph of the currents flowing in the cell body and pedicle of a single cone in response to voltage steps applied to the cell body. Along the abscissa is plotted the voltage command applied to the cell body. The ordinate represents the magnitude of the current flow in both the cell body and pedicle. The closer the two current values, the better coupled the two regions of the cell.

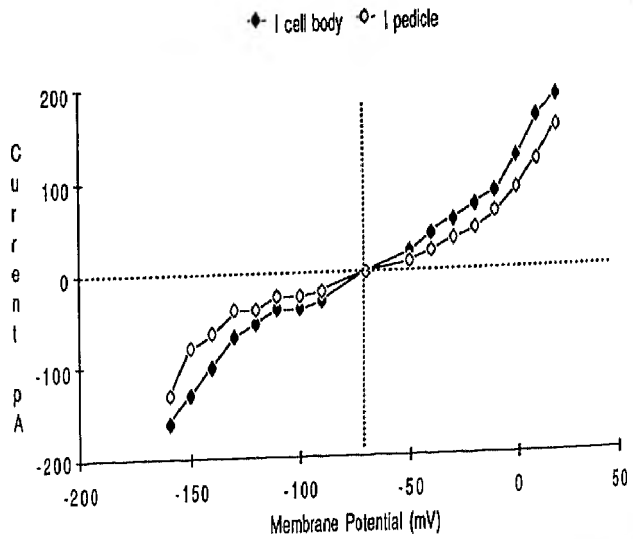

Fig. 5. The current-voltage relation for the pedicle and cell body membranes as determined with simultaneous voltage steps applied to both the pedicle and the cell body. Along the abscissa is plotted the clamped membrane potential and along the ordinate the magnitude of the current flow. The membrane responses are seen to rectify. The horizontal dotted line represents the zero current level and the vertical dotted line the holding potential. See text for details.

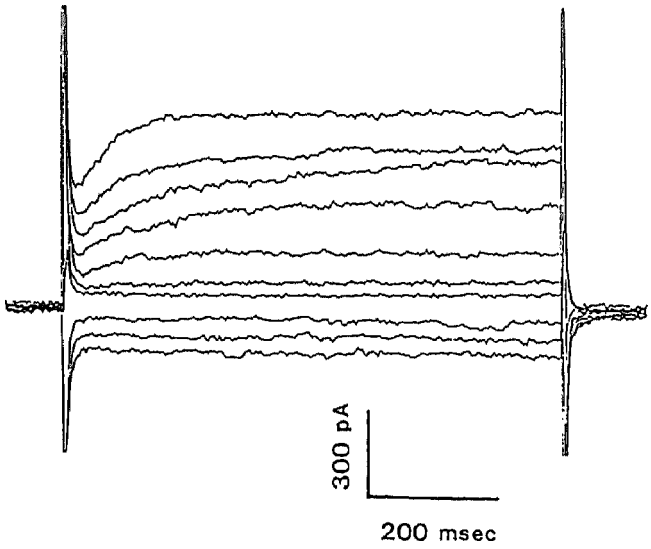

Fig. 6. Active membrane currents resulting from voltage clamping a cone cell body and pedicle in unison. Voltage commands were applied to cell body and pedicle simultaneously. The currents measured in the cell body in response to 20 mV incremental steps from −130 to +70 are plotted. The currents to depolarizing commands show a time-dependent activation. Holding potential = −70 mV.

Patch-clamp recordings of double cones. The simultaneous voltage-clamping technique described above was applied to double cones to investigate the coupling between principal and accessory members: one electrode was attached to the principal member and another was attached to the accessory member. In the nine double cones which were studied with two electrode whole-cell voltage-clamp technique, voltage steps in one member never evoked a measurable current response in the other member (Fig. 8). This was true for voltage stepping either the principal or the accessory cone. It is clear that in these isolated cones, the members of the double cone act in a totally autonomous fashion.

Discussion

Morphology and dimensions of cone photoreceptor axons in the turtle retina

The morphological studies were aimed at understanding the structure of the axon connecting the cell body and pedicle of the turtle cone, so that its role as a resistive element for information flow from the outer segment to the synaptic output point of the cell could be assessed. The axon length and diameter were also important dimensions to obtain for our calculations of signal propagation. The turtle photoreceptor axons appear to be homogeneous cytoplasm-filled structures with a scattering of synaptic vesicles and tubular cisternae in all photoreceptor types. The internal cell morphology appears to be consistent for all spectral types, and the diameters of axons seem to be uniform at 1–1.5 μm. However, the length of the axons can vary substantially. The most commonly occurring cones (red singles, green singles, and double cones) have axon lengths between 3 and 6 μm, while the rarer blue and putative UV-sensitive cone have mean axon lengths of 15 and 30 μm, respectively. In fact, we have observed the CC or UV-sensitive cones in cell culture with axons as long as 60 μm (Kolb & Jones, 1987). Thus, from these morphological findings, we might expect the commonest single cones and double cones of the turtle retina to act as isopotential units, but the blue and UV-sensitive cones might have an attenuation between cell body and pedicle allowing for a certain independence of the synaptic ending from the cell body.

Electrophysiological measurements of cytoplasmic resistivity in turtle single cones

The anatomical and electrophysiological results of this study can be combined to get a better estimate of the cytoplasmic resistivity of the cone. This resistivity, $\rho_{\text{cytoplasm}}$, can be obtained from the relation,

$$\rho_{\text{cytoplasm}} = (R_{\text{axon}} * \text{Area}_{\text{axon}})/\text{Length}_{\text{axon}}$$

where R_{axon} is the measured resistance of the axon, and $\text{Area}_{\text{axon}}$ and $\text{Length}_{\text{axon}}$ are cross-sectional area and length of the axon, respectively. When this equation was used to evaluate the cytoplasmic resistivity of each cone in this study, the mean resistivity was 33.7 (± 24.5 S.D., $n = 14$, range = 8–77) Ω-m, a surprisingly high value compared to the vertebrate cellular resistivities reported in the literature which are around 2 Ω-m (Schanne & Ruiz P.-Ceretti, 1978). Why this value for cytoplasmic resistivity is so high is not readily apparent. Several possibilities present themselves. For example, one might argue that if series resistance were not adequately compensated for, the magnitude of the voltage change at the clamp point is not known. The true value would be smaller than the attempted clamp value. This could, in fact, lead to an erroneous coupling resistance. In this case, however, the apparent resistance will be smaller than the actual resistance, not larger. One might also argue that a leaky cell body or pedicle membrane, resulting from the isolation procedure, might be the cause since some current could escape from the cell via this pathway. This cannot be the case, however, since due to the recording configuration, the unstepped electrode sees 100% of the current that flows through the axon. Even if the axon itself were leaky and we assumed that only 50% of the injected current was seen by the recording electrode, the apparent axon resistance and resulting cytoplasmic resistivity would still be very large. Finally, one might speculate that deterioration of the electrode-membrane seal might contribute to an artificially high axon resistance. This would be a problem also in measuring membrane resistance. The resistance would appear very low. This also is not the cause of our high resistivity values. In cells that showed very high input resistance, the cytoplasmic resistivity was still high.

So why do the axons of turtle cone photoreceptors have such high cytoplasmic resistivity? We suggest that the answer can be found by examining transverse sections through cone photoreceptors (i.e. Fig. 1B). In examining such a section, one notices that the nucleus of the cell sits directly over the expansion of the axon into the cell body. In most cases, there is very close apposition of the nuclear membrane to the plasma membrane, the distance between them being only 0.1 μm or less. In fact, the nucleus appears to fit into the neck of the axon much like a ball into a chalice or even a cork in a bottle. Since the nuclear envelope is expected to be relatively impermeable (Loewenstein, 1964), the nucleus fitting into the neck of the axon could restrict current flow and result in an apparent increase in

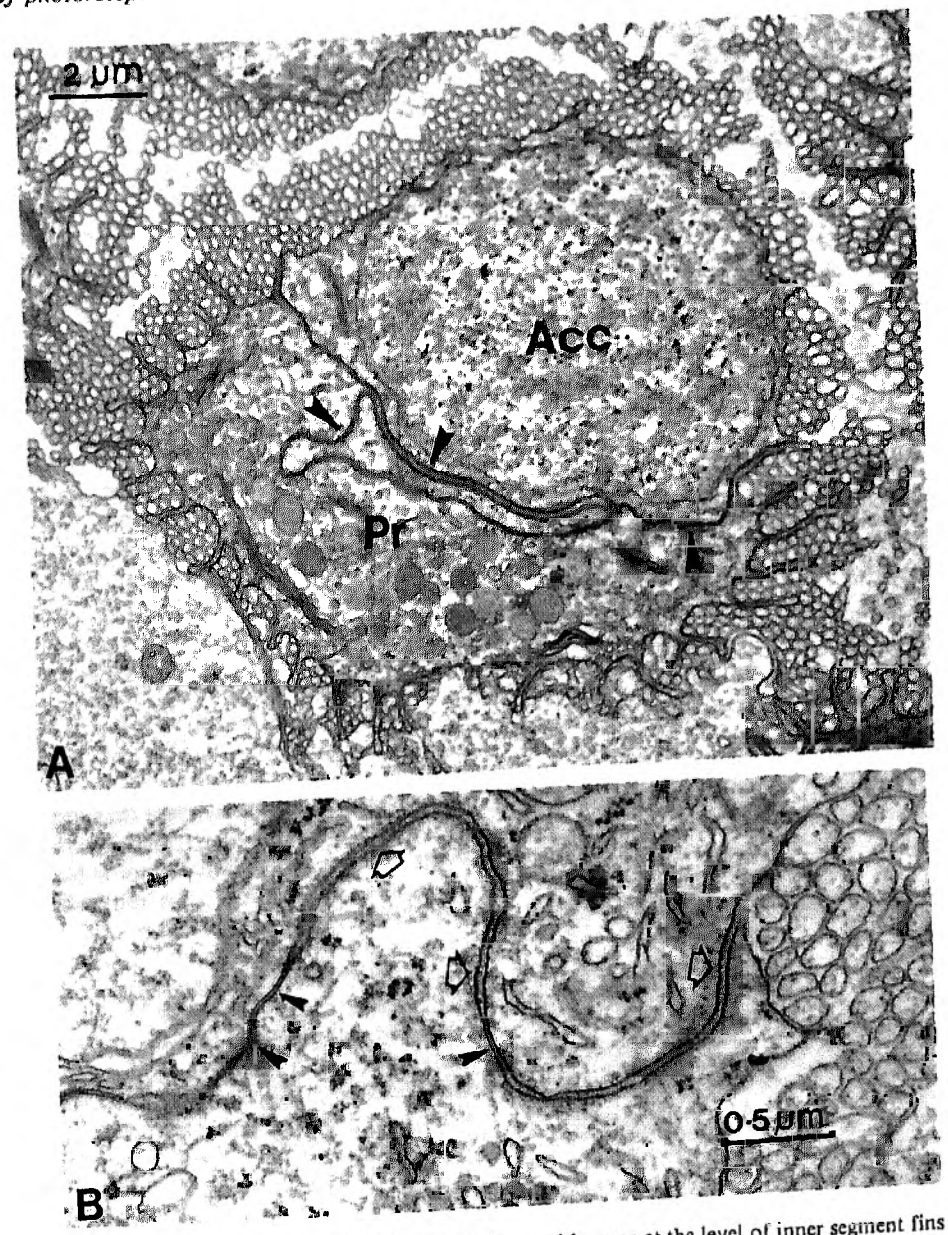

Fig. 7. A, electron micrograph of a tangential section through a double cone at the level of inner segment fins just above the outer limiting membrane. The principal (Pr) and accessory (Acc) members of the double cone are closely apposed and the membranes separating them are thrown into convolutions with an increased surface area (arrow heads). The nucleus of the accessory cone pokes up into the inner segment at this level of the double cone. Note the fins radiating from the sides of the cones and the interdigitating microvilli of the Müller cells projecting beyond the outer limiting membrane. Scale bar = 2 µm. B, higher magnification of the membranes between the two members of the double cones. Wide cleft portions of the membrane (open arrows) alternate with narrow cleft portions of the membrane appositions. The narrow cleft segments are closely enough aligned to be considered to be of gap junction-like proportions. Scale bar = 0.5 µm.

axonal resistance. Although this increase in resistance is not enough to electrically uncouple the cell body and pedicle regions of the cone, it is enough to raise the resistance of the axon and thus inflate values for cytoplasmic resistivity.

Signal propagation along a single cone

From published reports of the size of the typical maximal photoresponse of the turtle cone (recorded intracellularly) of about 25 mV (Baylor et al., 1971), and the 38 pA of maximal photocurrent recorded with suction electrodes applied around the outer segment of the turtle cone (Schnapf & McBurney, 1980), one would estimate that the net membrane resistance of the turtle cone should be about 660 MΩ. It is clear from our measurements of cone membrane resistances that some of our recordings may reflect damage due to the isolation procedure. Therefore, in the following analysis, we have selected only data from cones which manifested relatively high membrane resistances.

From the measured cell body and pedicle membrane resistances, and the axonal resistance of the single isolated cone, we can estimate the attenuation of signals as they are propagated from the cell body to the pedicle and from the pedicle to the

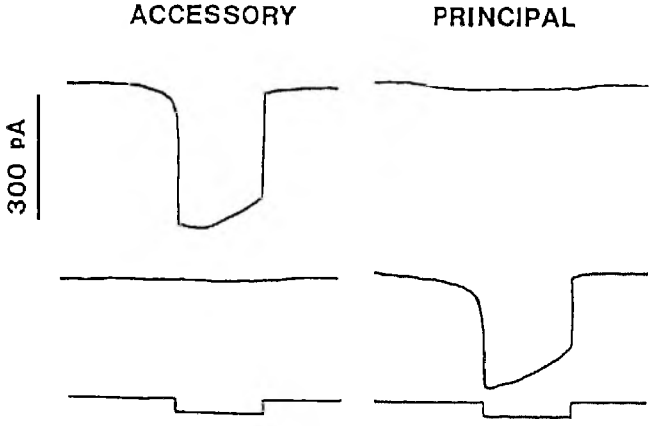

Fig. 8. Tracings of photographically reproduced responses showing lack of electrical coupling in double cones. Electrodes were placed in the principal and accessory members of a double cone and voltage commands applied alternately to each member. When the principal cone was stepped (bottom right trace) current flow was observed in the principal member (middle right trace) but not in the accessory member (middle left trace). Likewise, when the accessory member was stepped (bottom left trace), current flow was recorded in the accessory (top left trace) but not in the principal member (middle left trace). Command pulses were −70 mV and 100 msec

cell body. Based upon the caveat above, we have calculated data (based upon five photoreceptors) as most likely to represent the resistances of the isolated cone photoreceptor (Table 3).

Table 3. *Resistance of isolated cone photoreceptor (based upon 5 photoreceptors)*

Cell body resistance	1234 (± 242) MΩ
Pedicle resistance	1612 (± 895) MΩ
Longitudinal axonal resistance	35 MΩ[a]
Input impedance of isolated cone	700 MΩ[a]

[a]calculated.

From these values, signals recorded at the pedicle will be 98.6% of their amplitude at the cell body. Similarly, signals recorded at the cell body will be 97% of their amplitude at the pedicle. The average coupling coefficient of 0.888 (± 0.09 S.D., $n = 12$) supports this notion. It is clear from these estimates that even though the cone cytoplasm has an apparent high resistivity, the cone axon does not represent a significant barrier to the faithful propagation of information along the cone. We conclude, therefore, that the commonly encountered cone in the turtle retina can be considered to be relatively isopotential, and that synaptic events originating at the pedicle should be reflected in the cone cell body. Kraft and Burkhardt (1986) came to similar conclusions using a model of the pike perch cone. They estimated that 99% of the signal in the cell body should reach the pedicle, while about 83% of the signal in the pedicle should reach the cell body. Their model cone had an axon length of 36 μm and an axon diameter of 3 μm. They also assumed a cytoplasmic resistivity of 100 Ω-cm; a much smaller value than we measured experimentally. This adds further credence to the notion that our measured value is artificially inflated as described above. Exceptions to these findings were encountered with certain cones that had extremely long axons. These cones appeared to be the putative UV-sensitive cones. In them, the cell body, axonal and pedicle resistances were found to be comparable, and thus their pedicles could indeed be acting as independent summing points.

In light of the conclusion that the commonly occurring cones of the turtle retina, which are also most often recorded from intracellularly, are isopotential units, it is difficult to explain the differences in the surround effect seen in cones and bipolar cells in intracellular recordings in intact retina. It is possible that here we have improperly selected representative values for the resistances we have measured in isolated cones. The lower values of membrane resistance might be more representative. We regard this as being unlikely based upon the arguments discussed in the preceding section, and from the notion that the isolation procedure should have increased leakage conductances, not decreased them. Thus, the lack of a profound surround effect in cones more likely indicates that horizontal cells act not only on cones but also produce a direct inhibitory effect on the bipolar cells. Morphological studies of the turtle outer plexiform layer (Kolb & Jones, 1984) support this conclusion, as chemical synapses between H1 horizontal cell bodies and bipolar cell dendrites are fairly commonly encountered.

It is known that cones interact excitatorily with neighboring cones of like spectral class in the turtle retina (Baylor et al., 1971). These interactions probably result from the extensive gap junctions between telodendria which emerge from cone pedicle bases (Kraft & Burkhardt, 1986). In addition, we have evidence that cones interact in an excitatory manner with neighboring cones of differing spectral classes (at least in the turtle) (Normann et al., 1984, 1985). Thus, red cones receive an excitatory input from neighboring green cones which is probably mediated by chemical synapses from one spectral class of cone upon telodendria from neighboring cones of different spectral classes (Kolb & Jones, 1985). The physiological evidence for spectral mixing was obtained with intracellular microelectrodes most likely impaling cell bodies, yet clearly the synaptic effects at the cone pedicle were substantial enough to be seen. Again, this is consistent with our findings of low axonal resistance.

Double cones

Double cones in the turtle retina were originally believed to contain different photopigments as in the fish retina (Liebman & Granda, 1971). The very broad spectral sensitivities recorded in certain cones in turtle (Richter & Simon, 1974) were interpreted as being from double cones mediated by electrical coupling along the large appositional membrane area between these cones. Recent microspectrophotometric studies conducted by Lipetz and MacNichol (1982, 1983) and intracellular recordings done by Ohtsuka (1985*a*,*b*), however, provide compelling evidence that the outer segments of the principal and accessory members of the double cones contain the same red sensitive photopigment. Similar findings were shown for salamander double cones (Attwell et al., 1984) where both members contained 620-nm maximally sensitive photopigment. These recent findings raise the question of what function this large area of membrane apposition between the double cones can subserve and whether in fact the double cones are electrically coupled at all.

We present evidence in this paper that the inner segments of double cones do appear to have areas of narrow gaps between the membranes of the two apposed cones. Although it is dif-

ficult to be certain that these are indeed gap junctions without performing a freeze-fracture study, the ultrastructural appearance of these narrow gap segments are certainly suggestive of their being sites of small gap junctions. Interestingly, the inter narrow-gap segments of the double cone membranes are wider than commonly occurs between adjoining cell membranes. Furthermore, the whole surface area of the two apposed inner segments membranes appears to be increased by virtue of extensive infolding and convoluting. What the functional significance of this could be remains to be determined. The observation from our physiological measurements is that current injection in either the principal or the accessory member of the double cone has no effect on the other member. The principal and accessory members of double cones in salamander were seen not be coupled, as well (Attwell et al., 1984) when probed with two intracellular electrodes. It is possible that under the conditions of our experiments, the junctions were in a nonconducting state, possibly due to factors such as pH or intracellular calcium which are known to modify electrical coupling (Spray et al., 1984). However, pairs of fish horizontal cells (Lasater & Dowling, 1985) recorded under similar experimental conditions do show electrical coupling. On the other hand, it may be that while junctional conductance is intact, the junctional density is so low that appreciable amounts of current cannot flow between the cells. Nonetheless, our present results indicate that these two cells are not electrically coupled. This finding, together with the observation that each member of the double cone contains the same red-sensitive photopigment, raises the question of the significance of this class of photoreceptor in the turtle retina.

As double cones and twin cones with the same spectral sensitivity are observed in a large number of vertebrate retinas, they clearly must subserve some important functions, but the direct mixing of their color signals and specialized integration of spatial information do not seem to be one of these functions. Lipetz's interpretation (1985) for the turtle retina is that the double cones provide a basis for a second trivariant color circuit at the outer plexiform layer for animals such as birds and reptiles. The first circuit involves all the three or four (counting the UV-sensitive cones) single cones and an organized sequential circuit of inputs and feedback synapses to the three horizontal cell types and would be used over the color range of 400–700 nm. The second circuit involves the red single cone and the double cones and would function as a much more red-sensitive color discrimination circuit between cones and horizontal cells over a range of 550–700 nm.

We suggest that the findings of this paper on the turtle cones can be applied to the vertebrate photoreceptor in general. Thus, although other vertebrate retinas may not have double cones or ultraviolet-sensitive photoreceptors, for example, they all have single cones that appear very similar in morphology and dimensions to those of the turtle. Even cones of the primate and human peripheral retina are similar in size and shape to the single cones of the turtle retina. It is possible to suggest that the membrane properties and resistivities will in all likelihood be similar to those we report here for the common single cones of the turtle retina. A very interesting specialization of the human and primate retinas, though, is the extremely long cone photoreceptor of the foveal region of the retina. The so-called fibers of Henle are the axons of foveal cones which radiate out from the central fovea to terminate in pedicles concentrically arranged around the fovea. The lengths of the cone axons in this region of retina are as much as 500 μm (Boycott et al., 1986; Kolb, unpublished data). However, these axons are rather sturdy structures with diameters of 1.75 μm as measured from Golgi-stained cells in human retina (Kolb, unpublished). This is also the diameter of foveal cone inner segments in human and monkey retinas (Borwein et al., 1980; Kolb, unpublished). The findings presented in this paper on turtle cones suggests that the cones with long axons (one example with a 21-μm long axon, Table 2) may have axonal resistances of the same order of the cell body and the pedicle, and may thereby allow for some attenuation of the signal between the pedicle and the cell body. It is possible that this attenuation could be even more marked for a photoreceptor such as the foveal cone in the human retina.

Acknowledgments

This research was supported in part by Grants EY05972 (E.M.L.), EY03748 (R.A.N.), and EY04855 (H.K.), by an unrestricted grant to the Department of Ophthalmology from Research to Prevent Blindness (RPB) and by a Research Manpower Award from RPB to E.M.L.

References

Attwell, D., Werblin, F.S. & Wilson, M. (1982). The properties of single cones isolated from the tiger salamander retina. *Journal of Physiology* (London) **328**, 259–283.

Attwell, D., Wilson, M. & Wu, S.M. (1984). A quantitative analysis of interactions between photoreceptors in salamander (ambystoma) retina. *Journal of Physiology* (London) **352**, 703–737.

Baylor, D.A., Fuortes, M.G.F. & O'Bryan, P.M. (1971). Receptive field of cones in the retina of the turtle. *Journal of Physiology* (London) **214**, 265–294.

Borwein, B., Borwein, D., Medieros, J. & McGowan, J.W. (1980). The ultrastructure of monkey foveal photoreceptors, with special reference to the structure, shape, size, and spacing of the foveal cones. *American Journal of Anatomy* **159**, 125–146.

Boycott, B.B., Hopkins, J.M. & Sperling, H.G. (1986). Cone connections of the horizontal cells of the rhesus monkey. *Proceedings of the Royal Society B* **229**, 345–379.

Dalton, A.J. (1955). A chrome-osmium fixative for electron microscopy. *Anatomical Record* **121**, 281–287.

Hagins, W.A., Penn, R.D. & Yoshikami, S. (1970). Dark current and photocurrent in retinal rods. *Biophysical Journal* **10**, 380–412.

Hamill, O.P., Morty, A., Neher, E., Sakmann, B. & Segworth, F.J. (1981). Improved patch-clamp techniques for high-resolution recording from cells and cell-free membrane patches *Pfluegers Archiv* **391**, 85–100.

Kaneko, A. (1973). Receptive-field organization of bipolar and amacrine cells in the goldfish retina. *Journal of Physiology* (London) **235**, 133–153.

Kolb, H. & Jones, J. (1982). Light and electron microscopy of the photoreceptors in the retina of the red-eared slider (*Pseudemys scripta elegans*). *Journal of Comparative Neurology* **209**, 331–338.

Kolb, H. & Jones, J. (1984). Synaptic organization of the outer plexiform layer of the turtle retina: an electron microscope study of serial sections. *Journal of Neurocytology* **13**, 567–591.

Kolb, H. & Jones, J. (1985). Electron microscopy of Golgi-impregnated photoreceptors reveals connections between red and green cones in the turtle retina. *Journal of Neurophysiology* **54**, 304–317.

Kolb, H. & Jones, J. (1987). The distinction by light and electron microscopy of two types of cone containing colorless oil droplets in the retina of the turtle. *Vision Research* **27**, 1445–1458.

Kraft, T.W. & Burkhardt, D.A. (1986). Telodendrites of cone photoreceptors: structure and probable function. *Journal of Comparative Neurology* **249**, 13–27.

Lasater, E.M. & Dowling, J.E. (1985). Dopamine decreases conductance of the electrical junctions between cultured retinal horizontal cells. *Proceedings of the National Academy of Sciences of the U.S.A.* **82**, 3025–2029.

Liebman, P.A. & Granda, A.M. (1971). Microspectrophotometric measurements of visual pigments of two species of turtle, *Pseudemys scripta* and *Chelonia mydas*. *Vision Research* **11**, 105–114.

Lipetz, L.E. (1985). Some neuronal circuits of the turtle retina. In *The Visual System*, ed. Fein, A. & Levine, J.S., pp. 107–132. New York: Alan R. Liss.

Lipetz, L.E. & MacNichol, E.F., Jr. (1982). Photoreceptors of freshwater turtles: cell types and visual pigments. *Biological Bulletin* **163**, 396.

Lipetz, L.E. & MacNichol, E.F., Jr. (1983). Visual pigments of two freshwater turtles. *Biophysical Journal* **41** (2/2), 26a.

Loewenstein, W.E. (1964). Permeability of the nuclear membrane as determined with electrical methods. *Protoplasmatologia* **54**, 26–34.

Naka, K-I. & Nye, P.W. (1971). Role of horizontal cells in the organization of the catfish retinal receptive field. *Journal of Neurophysiology* **34**, 785–801.

Normann, R.A., Perlman, I., Kolb, H., Jones, J. & Daly, S.J. (1984). Direct excitatory interactions between cones of different spectral types in the turtle retina. *Science* **224**, 625–627.

Normann, R.A., Perlman, I. & Daly, S.J. (1985). Mixing of color signals by turtle cone photoreceptors. *Journal of Neurophysiology* **54**, 293–303.

Ohtsuka, T. (1985*a*). Relation of spectral types to oil droplets in cones of turtle retina. *Science* **229**, 874–877.

Ohtsuka, T. (1985*b*). Spectral sensitivities of seven morphological types of photoreceptors in the retina of the turtle (*Geoclemys reevesii*). *Journal of Comparative Neurology* **237**, 145–154.

Ohtsuka, T. & Kouyama, N. (1986). Electron-microscopic study of synaptic contacts between photoreceptors and HRP-filled horizontal cells in the turtle retina. *Journal of Comparative Neurology* **250**, 141–156.

Richter, A. & Simon, E.J. (1974). Electrical responses of double cones in the turtle retina. *Journal of Physiology* (London) **242**, 673–683.

Schanne, O.F. & Ruiz P.-Ceretti, E. (1978). *Impedance Measurements in Biological Cells*. Wiley Interscience.

Schnapf, J.L. & McBurney, R.N. (1980). Light-induced changes in membrane current in cone outer segments of tiger salamander and turtle. *Nature* **287**, 239–241.

Spray, D.C., White, R.L., Campos De Carvalho, A., Harris, A.L. & Bennett, M.V.L. (1984). Gating of gap junction channels. *Biophysical Journal* **45**, 219–230.

Toyoda, J.-I. & Kujiraoka, T. (1982). Analysis of bipolar cell responses elicited by polarization of horizontal cells. *Journal of General Physiology* **79**, 131–145.

Werblin, F.S. & Dowling, J.E. (1969). Organization of the retina of the mudpuppy, *Necturus maculosus*. II. Intracellular recording. *Journal of Neurophysiology* **32**, 339–355.